INTERNATIONAL JOURNAL OF ENERGY RESEARCH
*Int. J. Energy Res.* (2016)
Published online in Wiley Online Library (wileyonlinelibrary.com). DOI: 10.1002/er.3604

RESEARCH ARTICLE

# An assessment of the viability of hydrogen generation from the reaction of silicon powder and sodium hydroxide solution for portable applications

Paul Brack[1], S. E. Dann[1,*,†], K. G. U. Wijayantha[1], Paul Adcock[2] and Simon Foster[2]

[1]Energy Research Laboratory, Department of Chemistry, Loughborough University, Loughborough, Leicestershire LE11 3TU, United Kingdom
[2]Intelligent Energy Ltd, Charnwood Building, Holywell Park, Ashby Road, Loughborough, Leicestershire LE11 3GB, United Kingdom

## SUMMARY

The gravimetric hydrogen storage efficiency of silicon has been widely reported as 14 wt.%, suggesting that this material should be an excellent hydrogen generation source for portable applications. However, in the case of the reaction of silicon powder with 20 wt.% sodium hydroxide solution at 50 °C, the observed production of hydrogen fails to realize these high expectations unless a large excess of basic solution is used during the reaction, rendering the use of silicon in such systems uncompetitive compared with chemical hydride based technologies. By investigating the molar ratio of water:silicon from a large excess of water towards the stoichiometric 2:1 ratio dictated by the reaction equation, this study shows that for the reaction of silicon in 20 wt.% sodium hydroxide solution, the quantity of hydrogen produced decreases as the 2:1 ratio expected from the equation for the reaction is approached. Furthermore, in order to reach 80% of the theoretical efficacy, a molar ratio of 20:1, or 12 mL of 20 wt.% sodium hydroxide solution per gram of silicon, would be required. These results suggest that the actual gravimetric hydrogen storage capacity is less than 1%, casting doubts as to whether the use of silicon for hydrogen generation in real systems would be possible. © 2016 The Authors. *International Journal of Energy Research* published by John Wiley & Sons Ltd.

**KEY WORDS**

chemical hydrogen storage; silicon; hydrogen generation; hydrolysis

**Correspondence**

*S. E. Dann, Department of Chemistry, Loughborough University, Loughborough LE11 3TU, United Kingdom.
†E-mail: S.E.Dann@lboro.ac.uk



Received 4 November 2015; Revised 27 May 2016; Accepted 23 June 2016

## 1. INTRODUCTION

It is widely recognized that hydrogen has great potential as an energy vector [1–3]. Various methods to generate hydrogen have been studied in considerable depth, including electrolysis, photoelectrochemistry, fossil fuel reforming and artificial photosynthesis [4]. Because of its abundance in nature, water is an especially promising source of hydrogen, and many solar technologies have been developed to split water into hydrogen and oxygen using sunlight [5]. However, although hydrogen can be readily formed by such methods, it still remains difficult to store and transport because it has a very low density (0.0824 g $L^{-1}$ at 25 °C [6]). This is a particular issue for portable applications, where a high gravimetric hydrogen storage efficiency is required [7]. Thus, methods of splitting water into hydrogen and oxygen using chemicals with a higher density than hydrogen have become increasingly studied [8–12].

Silicon is considered to be an especially promising material for this type of application because of its high theoretical gravimetric hydrogen storage efficiency of 14 wt.% (although it should be noted that the hydrogen is obtained from the water with which the silicon reacts, rather than being stored in the silicon itself), low cost and abundance. As shown in Equations (1) and (2) [13,14], crystalline silicon reacts with water to form hydrogen. However, this process is severely retarded by the rapid formation of a thin film of silicon dioxide a few nanometers thick on the surface of silicon in the presence of air and moisture [15–17]. The rate of reaction of an untreated silicon powder with water is thus negligible unless some method of removing the oxide

layer is employed. The overall reaction of silicon with water has been described in previous work by Tichapondwa *et al.* [18,19] and is represented by Equations (1) and (2).

$$Si(cr) + 4\,H_2O(l) \rightarrow Si(OH)_4(aq) + 2\,H_2(g) \quad (1)$$

$$Si(cr) + 2\,H_2O(l) \rightarrow SiO_2(s) + 2\,H_2(g) \quad (2)$$

Nanosilicon has been shown to react much more rapidly with water than bulk silicon powders. For example, Erogbogbo *et al.* [13] synthesized 10-nm-diameter particles by laser pyrolysis and observed hydrogen generation rates 1000 times faster than for the reaction of silicon 325 mesh powders with water. This was primarily attributed to a change from an anisotropic etching process for bulk silicon to an isotropic process for nanosilicon. Foorde *et al.* have reported a process whereby nanosilicon is synthesized by ball milling of silicon 325 mesh powders [20,21]. The addition of a water soluble protective layer allows near instant evolution of hydrogen. However, the majority of these formulations suffered from poor percentage yields of hydrogen (<70%) because of the formation of the oxide layer on the silicon surface during the course of the reaction. Without an etchant to remove the oxide layer, the reactions were found to be self-limiting.

Reacting the silicon in an aqueous solution of an etchant such as sodium or potassium hydroxide serves to accelerate the onset of the hydrogen generation process by removal of the passivating oxide layer [22,23]. Reactions of silicon and hydroxides typically produce hydrogen at a faster rate than those of silicon or nanosilicon with water. The etch rates of silicon wafers in basic media have been studied extensively because of its widespread application in fields such as microelectrochemical systems (MEMS) [24–37]. The majority of these studies were conducted using cleaned (i.e. wafers from which the oxide layer had been removed by treatment with e.g. hydrofluoric acid) substrates with a specific crystallographic orientation of the silicon ((110), (100) or (111)). The overall reaction is typically expressed as shown in Equation (3) [38,39]:

$$Si(cr) + 2\,OH^-(aq) + 2\,H_2O(l) \rightarrow SiO_2(OH)_2^{2-}(aq) + 2\,H_2(g). \quad (3)$$

It should be noted that the nature of the hydroxide's role in the etching process (i.e. whether it behaves as a catalyst or as a stoichiometric reagent) has been controversial, but it is generally accepted that the water volume has a greater effect on the reaction rate than the hydroxide content. Shah *et al.* found that the etch rate of silicon (111) faces in 1–5 M solutions of KOH at 60 °C was independent of KOH concentration, but at lower alkaline concentrations, the etch rate of the silicon decreased with concentration [40]. From a detailed study of the etching of silicon (100) and (110) surfaces with potassium hydroxide, Seidel *et al.* deduced the following as the 'best fit' rate equation across the range of concentrations studied (10–60 wt.% KOH) [38]:

$$\text{Etch rate} = [H_2O]^4[KOH]^{0.25}. \quad (4)$$

The exact mechanism of the etching reaction depends on whether the silicon atoms at the surface are in a (110), (100) or (111) lattice plane, but the products of the reaction are the same. It has been reported that the surface atoms on silicon remain hydride terminated during the course of etching by hydroxide solutions [30]. Hydroxide ions and water are substituted for the surface hydrides, thus weakening the Si—Si back bonds and enabling the removal of surface silicon atoms in the form of silicates [41]. A postulated stepwise reaction scheme is shown in Scheme 1 [39], although various others also exist in the literature.

The (111) plane is the slowest etching as it requires the breaking of three Si—Si bonds rather than two [40,42]. The ratio of the etch rates for the different planes in potassium hydroxide was found to be 160:100:1 for (110)/(100)/(111) crystal planes at room temperature [38]. It is this variation in the etching rates that leads to the anisotropic etching observed with bulk silicon powders and silicon wafers [41].

However, it is noticeable that the studies of hydrogen generation from the reaction of hydroxide and silicon in the literature tend to focus on the concentration of the constituents of the etching solution; they do not take into account the effect of aqueous etchant solution volume. Indeed, such studies tend to use a large excess of etchant solution. However, the use of a large excess of aqueous etchant greatly reduces the gravimetric hydrogen storage density of the system, rendering silicon uncompetitive with respect to other chemical hydrogen generation materials such as lithium aluminium hydride ($LiAlH_4$), which are able to react with water vapour and without the need for etchants and thus maintain high gravimetric hydrogen storage densities [43–49]. In addition to the issues surrounding the reduced storage density, the design of systems to deliver significant quantities of etchant solution in a way to produce hydrogen consistently over an extended period is non-trivial.

If silicon is to be competitive as a chemical hydrogen storage material in terms of gravimetric hydrogen storage density, then the volume of water (and thus etchant solution) in the reaction must be reduced towards the stoichiometric amount (2 moles of water per mole of silicon). To our knowledge, the effect on the hydrogen yield of the reduction of the etchant solution volume has not been reported. Thus, in this work, we use an aqueous 20 wt.% sodium hydroxide–silicon hydrogen generation system as a model to investigate the effect of the reduction of the

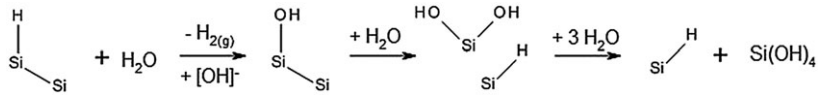


**Scheme 1.** Postulated mechanism for the etching of the Si (111) plane by the action of water and potassium hydroxide [39].

water volume towards stoichiometry on the hydrogen generation rate and yield.

## 2. EXPERIMENTAL

Silicon (99%, 325 mesh) and sodium hydroxide (reagent grade) were purchased from Sigma Aldrich and used as received. Deionized water was used to make up the solutions. The evolved hydrogen was collected and quantified using the water displacement method [10,50–54]. After preliminary experiments using various concentrations of sodium hydroxide, a 20 wt.% solution was chosen to enable experiments to be carried out in a reasonable timescale without a major induction period as a result of the need to remove the surface oxide layer. To investigate the effect of reducing the volume of 20 wt.% sodium hydroxide solution in the reaction, differing volumes of 20 wt.% sodium hydroxide solution were added to a 50-mL round bottomed flask and left to equilibrate at 50 °C for 10 min. To this was then added the desired amount of silicon, and the volume of hydrogen evolved recorded over a 10-min period. Each reaction was performed in triplicate. In order to identify the reaction byproducts, hydrochloric acid (reagent grade, 1 M) was added to the remaining reaction mixture until the solution pH was neutral, and the resulting gel left to dry under ambient conditions.

Powder X-ray diffraction (PXRD) data were collected on a Bruker D8 Discover diffractometer in transmission geometry using Co Kα radiation and a Braun linear position sensitive detector. Samples were mounted as powders on polymer tape. Data were collected over the 2θ range 15–95° with a step size of 0.007° 2θ and a count time of 1.0 s per step. X-ray photoelectron spectra were recorded using a VG Scientific Escalab Mk I instrument operating with a monochromatic Al Kα X-ray source (1486.6 eV). The particle size distribution was studied using a Leo 1530 VP field emission gun scanning electron microscope (FEG-SEM) at an accelerating voltage of 5 kV and a working distance of 12 mm. Particle size distributions were analysed using Zeiss' software package AxioVision 40 (V 4.8.2.0). IR spectra were collected on KBr pellets using a Shimadzu FTIR 8400S Spectrophotometer between 400 and 4000 $cm^{-1}$.

## 3. RESULTS AND DISCUSSION

### 3.1. Material characterization

The silicon powder used in these experiments was characterized using PXRD, X-ray photoelectron spectroscopy (XPS) and SEM. The PXRD pattern (Figure 1) shows reflections at 33.28, 55.62, 66.31, 82.53 and 91.82°2θ, which matches the database pattern (PDF 00-026-1481) for crystalline silicon (Cubic, Fd-3m (227)) and correspond to the (111), (220), (311), (400) and (331) planes, respectively. The sloping background is characteristic of the polymeric tape used to mount the sample. As expected, XPS of the

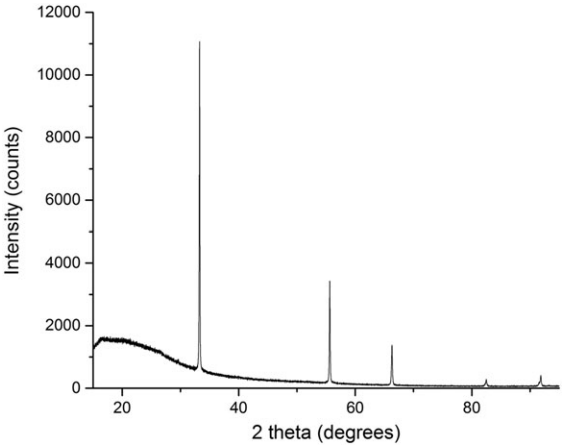


**Figure 1.** PXRD pattern of silicon 325 mesh powder collected over the 2θ range 15–95°.

Si 2p region (Figure 2) shows that the silicon powder is coated by a thin oxide layer (peaks at 99.28 and 103.38 correspond to Si and $SiO_2$ spectra in the NIST Database) [55,56]. The particle size distribution was analysed by SEM (Figures 3 and 4); the mean particle size was found to be 8.0 μm.

### 3.2. Hydrogen generation

In order to investigate the effect of reducing the volume of 20 wt.% sodium hydroxide solution on the yield of hydrogen, 0.20 and 0.30 g of silicon were reacted in different volumes of 20 wt.% sodium hydroxide solution ranging from 5 to 1 mL, and the volume of hydrogen evolved measured over a period of 10 min. The resulting hydrogen generation traces are shown in Figures 5 and 6. As has been observed before with reactions of partially passivated silicon powders, there is an induction period before the commencement of hydrogen evolution. This is because of the

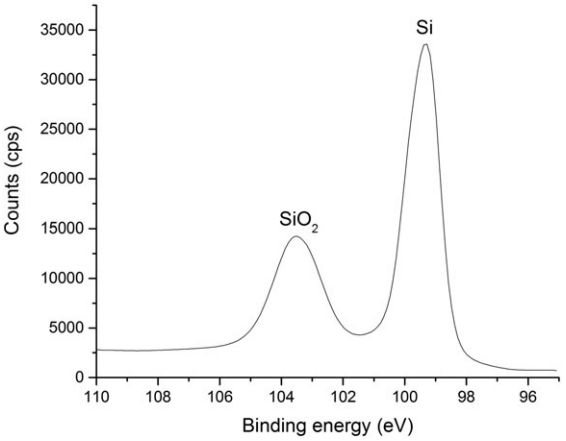


**Figure 2.** Si 2 p scan of silicon 325 mesh powder by XPS.

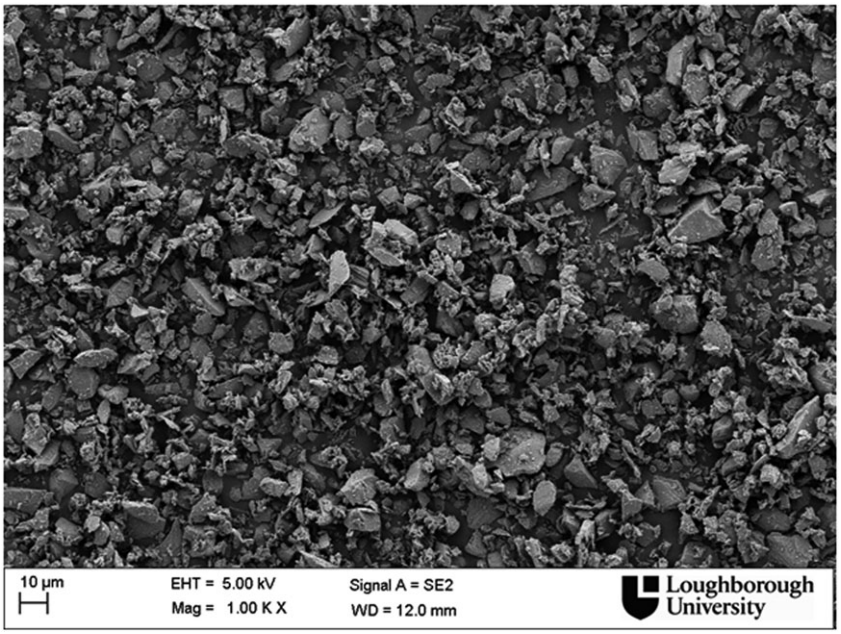


**Figure 3.** SEM image of the silicon 325 mesh powder used in this study.

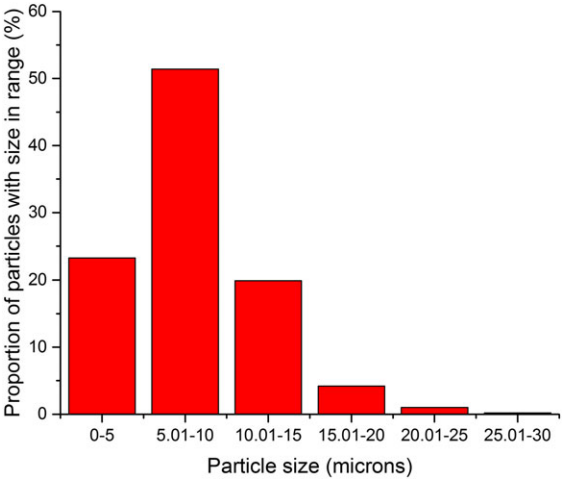


**Figure 4.** Particle size distribution of the silicon 325 mesh powder used in this study, obtained from the SEM image in Figure 3. Number of particles, *n*, = 502.

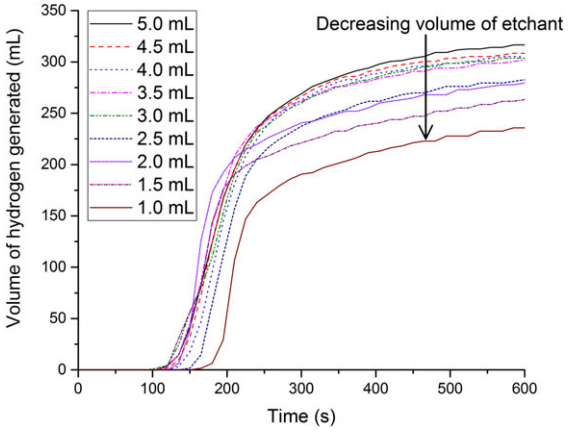


**Figure 5.** The volume of hydrogen generated as a function of time for the reaction of 0.20 g of silicon 325 mesh powder with 1.0, 1.5, 2.0, 2.5, 3.0, 3.5, 4.0, 4.5 and 5.0 mL of 20 wt.% sodium hydroxide solution at 50 °C.

etching of the surface silicon dioxide layer. As the rate of silicon dioxide etching, and thus the induction period of the hydrogen generation process, varies with etchant concentration, it was decided to keep the sodium hydroxide concentration constant in these reactions to ensure that any differences in the hydrogen generation curves are solely because of the variation of the volume of 20 wt.% sodium hydroxide solution. The initial stage of the hydrogen evolution reaction follows rapid kinetics, and it is in this stage that the majority of the hydrogen is evolved. For the reactions with 0.20 g of silicon powder (Figure 5), there is little change in the hydrogen generation profile from 5 to 3 mL, whereas for the reactions of 0.30 g of silicon powder, there is little change in the hydrogen generation profiles from 5 to 4 mL. For both, at lower volumes of 20 wt.% sodium hydroxide solution, the induction period is extended, and the initial hydrogen evolution rate is higher than at higher volumes of 20 wt.% sodium hydroxide solution. The higher rates are likely because of the smaller amount of 20 wt.% sodium hydroxide solution in which the heat of the reaction can be dissipated, resulting in a faster reaction.

Figures 7 and 8 illustrate the change in the percentage yield of hydrogen as the initial volume of 20 wt.% sodium hydroxide solution is reduced. When 0.20 g of silicon was used, the percentage yield remained relatively steady at

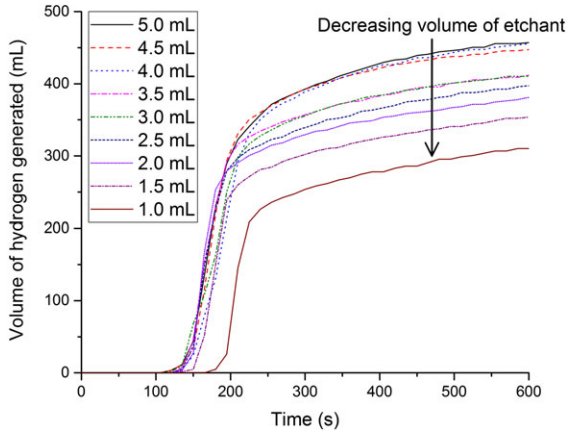


**Figure 6.** The volume of hydrogen generated as a function of time for the reaction of 0.30 g of silicon 325 mesh powder with 1.0, 1.5, 2.0, 2.5, 3.0, 3.5, 4.0, 4.5 and 5.0 mL of 20 wt.% sodium hydroxide solution at 50 °C.

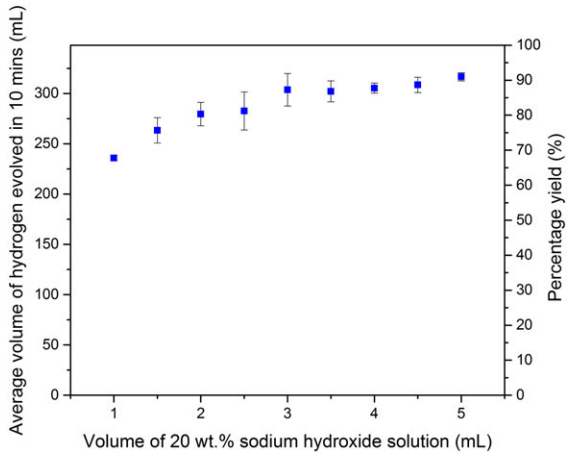


**Figure 7.** The total volume of hydrogen generated in 10 min and the percentage yield of hydrogen as a function of initial volume for the reaction of 0.20 g of silicon 325 mesh powder with varying volumes of 20 wt.% sodium hydroxide solution at 50 °C. The error bars show one standard deviation of the hydrogen evolution measurements.

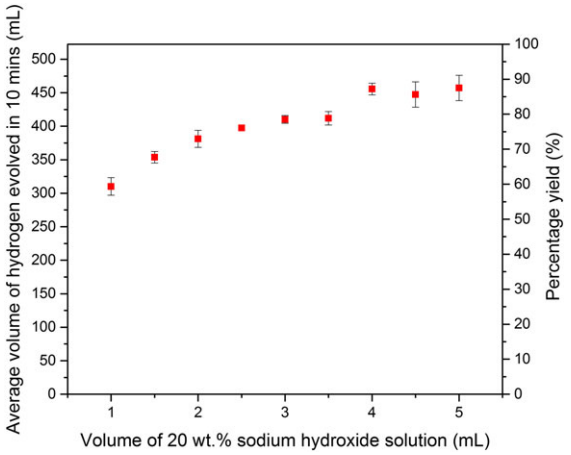


**Figure 8.** The total volume of hydrogen generated in 10 min and the percentage yield of hydrogen as a function of initial volume for the reaction of 0.30 g of silicon 325 mesh powder with varying volumes of 20 wt.% sodium hydroxide solution at 50 °C. The error bars show one standard deviation of the hydrogen evolution measurements.

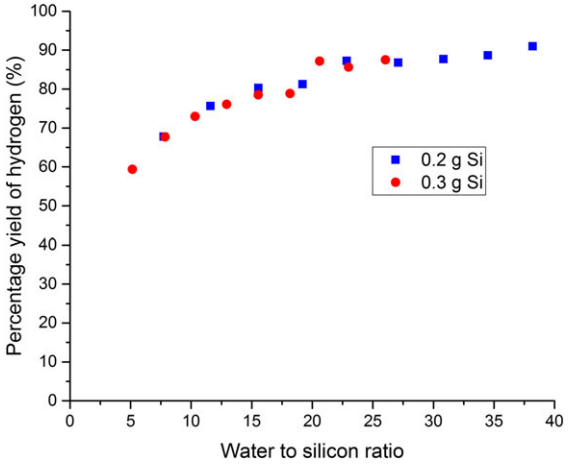


**Figure 9.** The variation of the percentage yield of hydrogen with initial water to silicon ratio for the reaction of 0.20 g (blue) and 0.30 g (red) of silicon 325 mesh powder with varying volumes of 20 wt.% sodium hydroxide solution at 50 °C.

~86–90% after 10 min for 3 to 5 mL of 20 wt.% sodium hydroxide solution, and then began to drop off sharply, falling to ~70% for 1 mL of 20 wt.% sodium hydroxide solution. A similar trend was observed with 0.30 g of silicon, except that the decrease in yield began at higher initial volumes of 20 wt.% sodium hydroxide solution and fell to ~60% when 1 mL was used.

The trend becomes even clearer when the percentage yield of hydrogen is plotted as a function of the initial water to silicon ratio rather than the volume of 20 wt.% sodium hydroxide solution (Figure 9). As the initial water to silicon molar ratio is reduced towards stoichiometry, the percentage yield of hydrogen reduces. Below ratios of ~20:1, the percentage yield of hydrogen decreases to values below 80%. Extrapolation of the graphs would suggest that at the stoichiometric water to silicon ratio of 2:1, the percentage yield of hydrogen would likely be <20%. Thus, to maintain reasonable yields of hydrogen (>80%), approximately 10 times the stoichiometric volume of 20 wt.% sodium hydroxide is required, i.e. a water to silicon ratio of 20:1, which equates to ~12 mL of 20 wt.% sodium hydroxide per gram of silicon. This corresponds to a gravimetric hydrogen storage density with respect to water and silicon of ~1 wt.%. Therefore, the actual gravimetric hydrogen storage capacity of such a system based on silicon and delivering hydrogen in high yields would be far lower than the theoretical value of ~14%.

The cause of this decrease in yield as the water to silicon ratio decreases is ascribed primarily to the formation of a viscous polysiloxane gel-like sludge on the surface

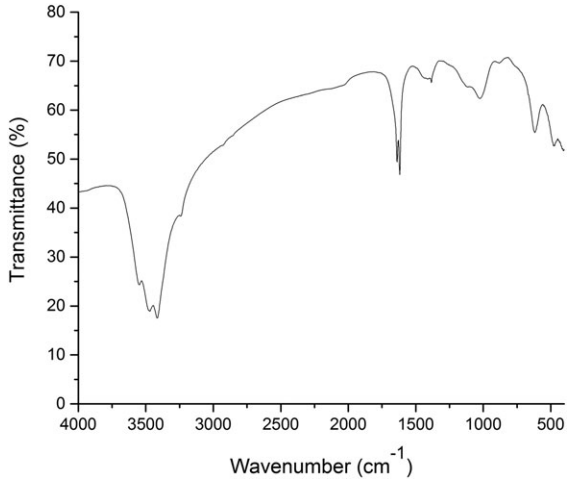


**Figure 10.** IR spectrum of the neutralized and dried reaction product collected on KBr pellets between 400 and 4000 $cm^{-1}$.

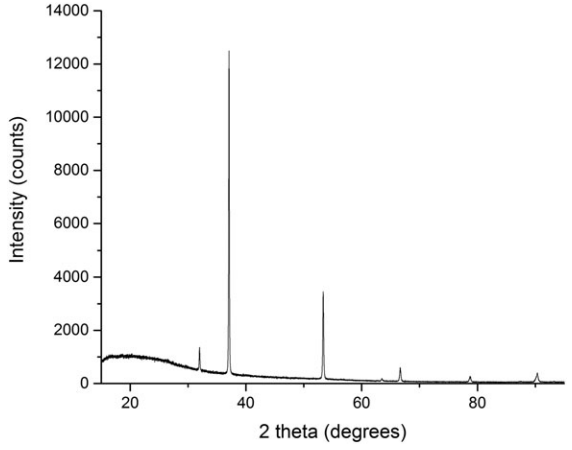


**Figure 11.** PXRD pattern of the neutralized and dried reaction product collected over the 2θ range 15–95°.

of the silicon powder which prevents efficient diffusion of sodium hydroxide solution to react with the silicon and also the efficient release of hydrogen gas as it is formed [31]. It is well known that silicate glasses can be formed by the reaction of sodium hydroxide with quartz ($SiO_2$) [57]. The higher the concentration of sodium hydroxide and quartz, the more viscous the solution becomes [57]. Thus, we propose that as the water volume is decreased, the hydrated sodium silicates formed as a by-product of the hydrogen generation reaction result in the solution becoming increasingly viscous, to the point where the remaining silicon is blocked from reaction because of the inability of free water molecules to efficiently penetrate the silicate glass and of hydrogen molecules formed from the water which does penetrate being impeded in their escape to the atmosphere. The relative decrease in hydroxide ion quantity with respect to silicon as the volume of 20 wt.% sodium hydroxide is reduced may also play a part in the build-up of an unsolubilized silicate layer on the surface, as according to Palik *et al*., hydroxide ions play a key role in the formation of soluble silicates in the reaction, and this process is retarded at low hydroxide concentrations [58].

To provide evidence for the formation of hydrated silicates in the reaction mixture, after the reaction was completed, the remaining sludge was neutralized by the addition of hydrochloric acid. At the point of neutralization, a white gel rapidly formed in an exothermic process. This gel was then dried and the obtained white powder subjected to analysis by FTIR and PXRD. The FTIR spectrum in Figure 10 confirms the presence of hydrated silicate by the presence of bands such as those at 1640 and 3300–3600 $cm^{-1}$ (O—H bending and stretching modes respectively), 3241 $cm^{-1}$ (Si—OH groups in structure amorphous silica), 1129 and 1022 $cm^{-1}$ (Si—O—Si asymmetric stretching vibrations), 882 $cm^{-1}$ (Si—O—Si symmetric stretching vibrations), 618 $cm^{-1}$ (Si—H) and 479 and 405 $cm^{-1}$ (O—Si—O bending vibrations) [56,59–64]. PXRD (Figure 11) confirms the amorphous nature of the silicate component, with all of the sharp reflections (31.95, 37.07, 53.32, 62.75, 66.56, 77.85 and 89.98°2θ) corresponding to crystalline sodium chloride (PDF 01-070-2509), formed as the excess sodium hydroxide was neutralized with hydrochloric acid.

## 4. CONCLUSIONS

The percentage yield of hydrogen generated by the reaction of silicon with water in 20 wt.% aqueous sodium hydroxide solution decreases as the molar ratio of water to silicon is decreased towards stoichiometry. Our study shows that ~12 mL of 20 wt.% sodium hydroxide solution is required per gram of silicon in order to achieve yields above 80%. Thus, the actual gravimetric hydrogen storage density of systems generating hydrogen by silicon hydrolysis would be much lower than the theoretical value of ~14%, and, as such, the deployment of bulk silicon powders in portable hydrogen generation devices would be problematic. As the volume of liquid needed to generate viable quantities of hydrogen would be significant, considerable weight and volume would be added to the device, thus reducing the practicality of making it portable in the first instance. These findings impact upon those endeavouring to develop *in situ* hydrogen generation methods for portable proton exchange membrane (PEM) hydrogen fuel cells.

## ACKNOWLEDGEMENTS

The authors would like to thank the EPSRC and Intelligent Energy Ltd for funding this project. PB would also like to thank the SCI for the award of a Messel Scholarship. The authors acknowledge use of the facilities and the assistance of Pat Cropper in the Loughborough Materials Characterisation Centre.

## REFERENCES


1. Schlapbach L, Züttel A. Hydrogen-storage materials for mobile applications. *Nature* 2001; **414**:353–358.
2. Hosseini SE, Wahid MA, Jamil MM, *et al.* A review on biomass-based hydrogen production for renewable energy supply. *International Journal of Energy Research* 2015; **39**:1597–1615.
3. Dincer I. Environmental and sustainability aspects of hydrogen and fuel cell systems. *International Journal of Energy Research* 2007; **31**:29–55.
4. Acar C, Dincer I. Impact assessment and efficiency evaluation of hydrogen production methods. *International Journal of Energy Research* 2015; **39**:1757–1768.
5. Turner J, Sverdrup G, Mann MK, *et al.* Renewable-hydrogen production. *International Journal of Energy Research* 2007; **32**:379–407.
6. Haynes WM (Ed). *CRC Handbook of Chemistry and Physics* (95th, 2014–15). CRC Press: Boca Raton, Florida, 2014.
7. Dalebrook AF, Gan W, Grasemann M, *et al.* Hydrogen storage: beyond conventional methods. *Chemical communications (Cambridge)* 2013; **49**(78):8735–8751.
8. Moussa G, Moury R, Demirci UB, *et al.* Boron-based hydrides for chemical hydrogen storage. *International Journal of Energy Research* 2013; **37**:825–842.
9. Brack P, Dann SE, Wijayantha KGU. Heterogeneous and homogenous catalysts for hydrogen generation by hydrolysis of aqueous sodium borohydride (NaBH4) solutions. *Energy Science & Engineering* 2015; **3**(3):174–188.
10. Brack P, Dann SE, Wijayantha KGU, *et al.* An old solution to a new problem? Hydrogen generation by the reaction of ferrosilicon with aqueous sodium hydroxide solutions. *Energy Science & Engineering* 2015; **3**(6):535–540.
11. Marrero-Alfonso EY, Beaird AM, Davis TA, Matthews MA. Hydrogen generation from chemical hydrides. *Industrial and Engineering Chemistry Research* 2009; **48**(8):3703–3712.
12. Weidenthaler C, Felderhoff M. Solid-state hydrogen storage for mobile applications: Quo Vadis? *Energy and Environmental Science* 2011; **4**(7):2495.
13. Erogbogbo F, Lin T, Tucciarone PM, *et al.* On-demand hydrogen generation using nanosilicon: splitting water without light, heat, or electricity. *Nano Letters* 2013; **13**(2):451–456.
14. Mehta RN, Chakraborty M, Parikh PA. Impact of hydrogen generated by splitting water with nano-silicon and nano-aluminum on diesel engine performance. *International Journal of Hydrogen Energy* 2014; **39**(15):8098–8105.
15. Mende G, Finster J, Flamm D, Schulze D. Oxidation of etched silicon in air at room temperature: measurements with ultrasoft X-ray photoelectron spectroscopy (ECSA) and neutron activation analysis. *Surface Science* 1983; **128**:169–175.
16. Morita M, Ohmi T, Hasegawa E, *et al.* Control factor of native oxide growth on silicon in air or in ultrapure water. *Applied Physics Letters* 1989; **55**(6):562–564.
17. Morita M, Ohmi T, Hasegawa E, *et al.* Growth of native oxide on a silicon surface. *Journal of Applied Physics* 1990; **68**(3):1272.
18. Tichapondwa SM, Focke WW, Del Fabbro O, *et al.* Suppressing $H_2$ evolution by silicon powder dispersions. *Journal of Energetic Materials* 2011; **29**(4):326–343.
19. Tichapondwa SM, Focke WW, Fabbro OD, *et al.* Suppressing hydrogen evolution by aqueous silicon powder dispersions through the introduction of an additional cathodic reaction. *Chemical Engineering Communications* 2014; **201**(4):501–515.
20. Foord, JS, and Ashraf, S (2011) Preparation of silicon for fast generation of hydrogen through reaction with water. WO 2011/058317, issued 2011.
21. Foord, JS, and Hu, J (2014) Composition for hydrogen generation. WO 2014/053799, issued 2014.
22. Palik ED, Gray HF, Klein PB. A Raman study of etching silicon in aqueous KOH. *Journal of the Electrochemical Society* 1983; **130**(4):956–959.
23. Dai F, Zai J, Yi R, *et al.* Bottom-up synthesis of high surface area mesoporous crystalline silicon and evaluation of its hydrogen evolution performance. *Nature Communications* 2014; **5**:3605.
24. Haiss W, Raisch P, Bitsch L, *et al.* Surface termination and hydrogen bubble adhesion on Si(100) surfaces during anisotropic dissolution in aqueous KOH. *Journal of Electroanalytical Chemistry* 2006; **597**(1):1–12.
25. Haiss W, Raisch P, Schiffrin DJ, *et al.* An FTIR study of the surface chemistry of the dynamic Si (100) surface during etching in alkaline solution. *Faraday Discussions* 2002; (100):167–180.
26. Kelly JJ, Philipsen HGG. Anisotropy in the wet-etching of semiconductors. *Current Opinion in Solid State and Materials Science* 2005; **9**(1–2):84–90.
27. Philipsen HGG, Kelly JJ. Influence of chemical additives on the surface reactivity of Si in KOH solution. *Electrochimica Acta* 2009; **54**(13):3526–3531.
28. Shah IA, Nguyen QD, Philipsen HGG, *et al.* X-ray diffraction analysis of the silicon (111) surface during alkaline etching. *Surface Science* 2011; **605**(11–12):1027–1033.
29. Wind RA, Jones H, Little MJ, Hines MA. Orientation-resolved chemical kinetics: using microfabrication to unravel the complicated chemistry of KOH/Si


 
DOI: 10.1002/er

etching. *The Journal of Physical Chemistry. B* 2002; **106**(7):1557–1569.
30. Rappich J, Lewerenz HJ, Gerischer H. The surface of Si(111) during etching in NaOH studied by FTIR spectroscopy in the ATR technique. *Journal of the Electrochemical Society* 1993; **140**(12):L187–L189.
31. Garcia S, Bao H, Hines M. Etchant anisotropy controls the step bunching instability in KOH etching of silicon. *Physical Review Letters* 2004; **93**(16):166102.
32. Glembocki OJ, Palik ED, Deguel GR, Kendall DL. Hydration model for the molarity dependence of the etch rate of Si in aqueous alkali hydroxides. *Journal of the Electrochemical Society* 1991; **138**(4):1055–1063.
33. Shah IA, van der Wolf BMA, van Enckevort WJP, Vlieg E. Wet chemical etching of silicon {111}: autocatalysis in pit formation. *Journal of the Electrochemical Society* 2008; **155**(3):J79.
34. Allongue P. Etching of silicon in NaOH solutions. *Journal of the Electrochemical Society* 1993; **140**(4):1018.
35. Baum T, Schiffrin DJ. Mechanistic aspects of anisotropic dissolution of materials etching of single-crystal silicon in alkaline solutions. *Journal of the Chemical Society, Faraday Transactions* 1998; **94**(5):691–694.
36. Baum T, Schiffrin DJ. Kinetic isotopic effects in the anisotropic etching of p-Si〈100〉 in alkaline solutions. *Journal of Electroanalytical Chemistry* 1997; **436**(1–2):239–244.
37. Philipsen HGG, Kelly JJ. Anisotropy in the anodic oxidation of silicon in KOH solution. *The Journal of Physical Chemistry. B* 2005; **109**(36):17245–17253.
38. Seidel H, Csepregi L, Heuberger A, Baumgartel H. Anisotropic etching of crystalline silicon in alkaline solutions. *Journal of the Electrochemical Society* 1990; **137**(11):3612–3626.
39. Shah IA, Koekkoek AJJ, van Enckevort WJP, Vlieg E. Influence of additives on alkaline etching of silicon(111). *Crystal Growth and Design* 2009; **9**(10):4315–4323.
40. Shah IA, van Enckevort WJP, Vlieg E. Absolute etch rates in alkaline etching of silicon (111). *Sensors and Actuators, A: Physical* 2010; **164**(1–2):154–160.
41. González-Pereyra NG, Glasgow W, Parenzan A, *et al.* Investigation of the etching of silicon under subcritical water conditions. *Industrial and Engineering Chemistry Research* 2014; **53**(1):173–181.
42. Jiang Y, Huang Q. A physical model for silicon anisotropic chemical etching. *Semiconductor Science and Technology* 2005; **20**(6):524–531.
43. Moghaddam S, Pengwang E, Lin KY, *et al.* Millimeter-scale fuel cell with onboard fuel and passive control system. *Journal of Microelectromechanical Systems* 2008; **17**(6):1388–1395.
44. Zhu L, Kim D, Kim H, *et al.* Hydrogen generation from hydrides in millimeter scale reactors for micro proton exchange membrane fuel cell applications. *Journal of Power Sources* 2008; **185**(2):1334–1339.
45. Moghaddam S, Pengwang E, Masel RI, Shannon MA. A self-regulating hydrogen generator for micro fuel cells. *Journal of Power Sources* 2008; **185**(1):445–450.
46. Zhu L, Swaminathan V, Gurau B, *et al.* An onboard hydrogen generation method based on hydrides and water recovery for micro-fuel cells. *Journal of Power Sources* 2009; **192**(2):556–561.
47. Moghaddam S, Pengwang E, Masel RI, Shannon M. An enhanced microfluidic control system for improving power density of a hydride-based micro fuel cell. *Journal of Power Sources* 2010; **195**(7):1866–1871.
48. Eickhoff S, Zhang C, Cui T. Micro fuel cell utilizing fuel cell water recovery and pneumatic valve. *Journal of Power Sources* 2013; **240**:1–7.
49. Eickhoff S, Zhang C, Cui T. The effects of hydride chemistry, particle size, and void fraction on micro fuel cell performance. *Journal of Power Sources* 2013; **243**:562–568.
50. Teprovich JA, Motyka T, Zidan R. Hydrogen system using novel additives to catalyze hydrogen release from the hydrolysis of alane and activated aluminum. *International Journal of Hydrogen Energy* 2012; **37**(2):1594–1603.
51. Seven F, Sahiner N. Enhanced catalytic performance in hydrogen generation from $NaBH_4$ hydrolysis by super porous cryogel supported Co and Ni catalysts. *Journal of Power Sources* 2014; **272**:128–136.
52. Saha S, Basak V, Dasgupta A, *et al.* Graphene supported bimetallic G–Co–Pt nanohybrid catalyst for enhanced and cost effective hydrogen generation. *International Journal of Hydrogen Energy* 2014; **39**:11566–11577.
53. Demirci S, Sahiner N. Superior reusability of metal catalysts prepared within poly (ethylene imine) microgels for $H_2$ production from $NaBH_4$ hydrolysis. *Fuel Processing Technology* 2014; **127**:88–96.
54. Brack P, Dann SE, Wijayantha KGU, *et al.* A simple, low-cost, and robust system to measure the volume of hydrogen evolved by chemical reactions with aqueous solutions. *Journal of Visualized Experiments*, (In press) 2016.
55. Kanungo J, Maji S, Mandal AK, *et al.* Surface treatment of nanoporous silicon with noble metal ions and characterizations. *Applied Surface Science* 2010; **256**(13):4231–4240.

56. Zhan C, Chu PK, Ren D, *et al.* Release of hydrogen during transformation from porous silicon to silicon oxide at normal temperature. *International Journal of Hydrogen Energy* 2011; **36**(7):4513–4517.
57. Lagaly G, Tufar W, Minihan A, Lovell A. Silicates. *Ullmann's Encyclopedia of Industrial Chemistry* 2000:509–569.
58. Palik ED, Bermudez VM, Glembocki OJ. Ellipsometric study of orientation-dependent etching of silicon in aqueous KOH. *Journal of the Electrochemical Society* 1985; **132**(4):871.
59. Music S, Filipovic-Vincekovic N, Sekanovic L. Precipitation of amorphous $SiO_2$ particles and their properties. *Brazilian Journal of Chemical Enginering* 2011; **28**(01):89–94.
60. Agarwal A, Tomozawa M. Correlation of silica glass properties with the infrared spectra. *Journal of Non-Crystalline Solids* 1997; **209**:166–174.
61. Husung RD, Doremus RH. The infrared transmission spectra of four silicate glasses before and after exposure to water. *Journal of Materials Research* 1990; **5**:2209–2217.
62. Kale P, Gangal AC, Edla R, Sharma P. Investigation of hydrogen storage behavior of silicon nanoparticles. *International Journal of Hydrogen Energy* 2012; **37**(4):3741–3747.
63. Lysenko V, Bidault F, Alekseev S, *et al.* Study of porous silicon nanostructures as hydrogen reservoirs. *The Journal of Physical Chemistry. B* 2005; **109**(42):19711–19718.
64. Manilov AI, Alekseev SA, Skryshevsky VA, *et al.* Influence of palladium particles impregnation on hydrogen behavior in meso-porous silicon. *Journal of Alloys and Compounds* 2010; **492**(1–2):466–472.

 
DOI: 10.1002/er